Stable high-dimensional spatial weak-light solitons in a resonant three-state atomic system

Chao Hang and Guoxiang Huang*
Department of Physics, East China Normal University, Shanghai 200062, China

L. Deng
Electron and Optical Physics Division, NIST, Gaithersburg, Maryland 20899, USA

(Received 6 March 2006; published 3 October 2006)

We study the formation of a nonlinear localized high-dimensional optical beam in a lifetime-broadened three-state atomic system. We show that stable high-dimensional spatial optical solitons with extremely weak-light intensity can occur in such a highly resonant medium through a mechanism of electromagnetically induced transparency. We demonstrate that the interaction between two high-dimensional spatial optical solitons displays interesting properties and these solitons can be easily controlled by manipulating the coupling optical field of the system.

DOI: 10.1103/PhysRevE.74.046601 PACS number(s): 42.81.Dp, 42.65.Tg, 05.45.Yv, 42.50.Gy

I. INTRODUCTION

Optical solitons have been the subject of intensive theoretical and experimental studies in recent years [1–3]. Spatial-optical solitons are localized optical beams that form in optical media when the combined effects of refractive nonlinearity and beam diffraction can compensate each other. There are many useful properties for the spatial optical solitons, which are promising for practical applications in optical information processing and engineering [2–4]. However, in conventional methods of generating spatial optical solitons, optical fields far away from atomic resonances are used in order to avoid a large absorption of media. Thus for obtaining significant nonlinearity that balances diffraction, highly intense lights are needed.

In recent years, much attention has been paid to the investigation on electromagnetically induced transparency (EIT) in highly resonant optical media [5]. By means of the quantum interference effect induced by a coupling laser field, the absorption of a probe laser field tuned to a strong one-photon resonance can be largely suppressed and hence an initially highly opaque optical medium becomes transparent. The wave propagation in the optical medium under EIT configuration displays many striking features. One of them is the significant enhancement of Kerr nonlinearity, which is beneficial to certain nonlinear optical processes under weak driving conditions [5–9]. Based on these features, it has been shown that spatial optical solitons with a weak-light intensity can occur in a four-level atomic system [10,11]. In addition, in EIT media the temporal-optical solitons that have ultraslow propagating velocity, i.e., ultraslow optical solitons, have also been predicted recently in various highly resonant optical media [12–14]. Due to very low-light intensity and the robust property during propagation, such optical solitons have potential applications in quantum information processing [10–14].

In this work, we shall study the formation and propagation of spatial optical solitons in a resonant three-state atomic system under a mechanism of EIT. Different from the four-state system used in Refs. [10,11], our scheme is simple and requires less physical resources. In addition, the probe optical field in our system is governed by a nonlinear Schrödinger (NLS) equation with much simpler saturation nonlinearity. Furthermore, in our work the stability of (2+1)-dimensional [(2+1)-D] spatial optical solitons is studied by using the Vakhitov-Kolokolov (VK) criterion [15]. The property of the interaction between two spatial solitons is investigated in detail. We shall also present a numerical simulation for the (2+1)-D spatial soliton starting directly from Maxwell-Schrödinger equations that control the evolution of atomic amplitudes and the probe field. The paper is arranged as follows. In Sec. II we describe the three-level atomic model and derive the nonlinear equation governing the motion of the envelope of the probe field and discuss its solution in linear regime. In Sec. III we present (2+1)-D spatial-optical soliton solutions and study their stability. The controllability of the spatial optical solitons by manipulating the coupling field is also discussed. Finally, Sec. IV contains a summary of our main results.

II. MODEL AND SOLUTION IN LINEAR REGIME

We consider a lifetime-broadened three-level, gaseous atomic system, which interacts with a weak, pulsed probe field of central frequency $\omega_p/(2\pi)$ ($|1\rangle \rightarrow |3\rangle$ transition) and a strong, continuous-wave coupling field of frequency $\omega_c/(2\pi)$ ($|2\rangle \rightarrow |3\rangle$ transition), respectively (see Fig. 1). The electric-field vector of the system can be written as $\mathbf{E}=\Sigma_{l=p,c}\mathbf{e}_l\mathcal{E}_l \exp[i(k_l z-\omega_l t)]+\text{c.c.}$, where $\mathbf{e}_p$ ($\mathbf{e}_c$) is the unit vector denoting the polarization of the probe (coupling) laser field, with the envelope $\mathcal{E}_p$ ($\mathcal{E}_c$). The Hamiltonian of the system is given by $\hat{H}=\hat{H}_0+\hat{H}'$, where $\hat{H}_0$ describes a free atom and $\hat{H}'$ describes the interaction between the atom and the electric field, respectively. In the Schrödinger picture, the state vector of the system is $|\Psi(t)\rangle=\Sigma_{j=1}^{3}c_j(x,y,z,t)|j\rangle$, where $|j\rangle$ is the eigenvector of $\hat{H}_0$. In a rotating-wave approximation, the Hamiltonian reads

*Author to whom correspondence should be address. Electronic address: gxhuang@phy.ecnu.edu.cn

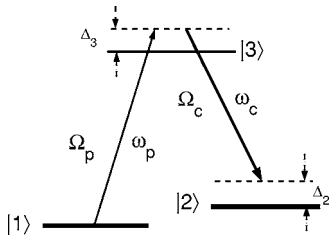

FIG. 1. Energy-level diagram and excitation scheme of a lifetime-broadened three-state atomic system, which interacts with a weak, pulsed probe field of central frequency $\omega_p/(2\pi)$ and a strong, continuous-wave (cw) control field of frequency $\omega_c/(2\pi)$.

$$H = \sum_{j=1}^{3} \hbar\,\omega_j |j\rangle\langle j| - \hbar\,(\Omega_p^* e^{i(k_p z-\omega_p t)}|1\rangle\langle 3| + \Omega_c^* e^{i(k_c z-i\omega_c t)}|2\rangle\langle 3| + \text{H.c.}), \tag{1}$$

where $\hbar\omega_j$ is the energy of state $|j\rangle$, $\Omega_p = \mathbf{e}_p \cdot \mathbf{p}_{31}\mathcal{E}_p/\hbar$ ($\Omega_c = \mathbf{e}_c \cdot \mathbf{p}_{32}\mathcal{E}_c/\hbar$) is the half Rabi frequency corresponding to the probe (coupling) optical field, with $\mathbf{p}_{ij}$ being the electric-dipole matrix element associated with the transition from $|j\rangle$ to $|i\rangle$.

To investigate the time evolution of the system it is more convenient to employ an interaction picture, which is obtained by making the transformation $c_j(x,y,z,t) = A_j(x,y,z,t)\exp[i(k_j z-\omega_j t)]$, with $k_1=0$, $k_2=k_p-k_c$, and $k_3=k_p$. The Hamiltonian in the interaction picture is given by

$$H_{\text{int}} = -\hbar \sum_{j=2}^{3} \Delta_j |j\rangle\langle j| - \hbar\,(\Omega_p|3\rangle\langle 1| + \Omega_c|3\rangle\langle 2| + \text{H.c.}), \tag{2}$$

where Δ_2 and Δ_3 are, respectively, the two- and one-photon detunings between the states $|1\rangle \to |2\rangle$ and $|1\rangle \to |3\rangle$, i.e., $\Delta_2 = \omega_p - \omega_c - (\omega_2 - \omega_1)$ and $\Delta_3 = \omega_p - (\omega_3 - \omega_1)$. Based on the Schrödinger equation, the equations of motion for the atomic probability amplitude A_j take the following form:

$$\left(i\frac{\partial}{\partial t} + d_2\right)A_2 + \Omega_c^* A_3 = 0, \tag{3a}$$

$$\left(i\frac{\partial}{\partial t} + d_3\right)A_3 + \Omega_p A_1 + \Omega_c A_2 = 0, \tag{3b}$$

together with the condition $\Sigma_{j=1}^{3}|A_j|^2 \approx 1$, where $d_j = \triangle_j + i\gamma_j^{\text{AV}}$ ($j=2,3$; AV=amplitude variable), with γ_j^{AV} being the decay rate of the state $|j\rangle$. We assume that the system is partially open, i.e., the influence of the nearby levels is taken into account by γ_j^{AV}, which are introduced phenomenologically in the model (3) [16]. The initial state of the system is in the ground state $|1\rangle$, i.e., $A_1=1$, $A_2=A_3=0$ at $t=0$. Notice that if the intensity of the probe field Ω_p is much weaker than that of the coupling field Ω_c, due to the quantum coherence and interference (i.e., EIT) effect the depletion of the ground state $|1\rangle$ is not significant and hence one has $A_1 \approx 1$ for any $t>0$ [16].

The equation of motion for $\Omega_p(x,y,z,t)$ can be obtained by the Maxwell equation

$$\nabla^2\mathbf{E} - \frac{1}{c^2}\frac{\partial^2\mathbf{E}}{\partial t^2} = \frac{1}{\varepsilon_0 c^2}\frac{\partial^2\mathbf{P}}{\partial t^2}, \tag{4}$$

with $\mathbf{P} = \mathcal{N}_a \Sigma_{j=1,2}[\mathbf{p}_{j3}A_3 A_j^* \exp[i(k_j z-\omega_j t)] + \text{c.c.}]$. Under a slowly varying envelope approximation, Eq. (4) is reduced to

$$i\left(\frac{\partial}{\partial z} + \frac{1}{c}\frac{\partial}{\partial t}\right)\Omega_p + \frac{c}{2\omega_p}\left(\frac{\partial^2}{\partial x^2} + \frac{\partial^2}{\partial y^2}\right)\Omega_p + \kappa A_3 A_1^* = 0, \tag{5}$$

where the propagation coefficient $\kappa = \mathcal{N}_a\omega_p|\mathbf{p}_{13}|^2/(2\varepsilon_0\hbar c)$, with $\mathcal{N}_a$ being the atomic density and c being the light speed in vacuum. We assume that the coupling field is strong enough and not depleted so that Ω_c can be taken as a constant.

Notice that in the present work we employ the amplitude variable (AV) approach [i.e., Eq. (3)] for the description of the motion of atoms. Strictly speaking, for a lifetime-broadened system, a density-matrix equation approach should be used in order to get a complete description to include spontaneous emission and dephasing. However, for an EIT-based partially open system, it can be shown that two approaches are roughly equivalent. The main reason for such equivalence is due to the fact that the coupling field Ω_c induces a quantum coherence in the system and suppresses the spontaneous emission greatly. The dominant processes in the system are hence coherent, reversible transitions between the hyperfine ground states. The quantity, which determines the importance of the incoherent processes, is given by the fraction of the population undergoing spontaneous emission integrated over time,

$$P_{\text{loss}} = \gamma_3^{\text{AV}} \int_0^\infty dt|A_3(t)|^2, \tag{6}$$

which we will show later (see the end of Sec. III A) is indeed small. For detailed discussions, we refer to Refs. [16,17]. In Appendix A, we have presented the equations of motion for the density matrix of our system and given the relations between the decay rate γ_j^{AV} in the AV equations (3) and the spontaneous emission decay rates and dephasing rates in the density matrix equations (A1). Another reason for the choice of the AV approach is due to its simplicity in mathematical treatment and its transparency in the physical explanation of the results obtained [12–14,16–18].

We are interested in an adiabatic regime in which the envelope of the probe optical pulse varies slowly with respect to time so that an atomic response can follow the variation of the probe field adiabatically. In this regime the time-derivative terms in Eqs. (3a) and (3b) can be safely neglected [19]. Under such an approximation, by Eq. (3) we get $A_1 = 1/[1+W|\Omega_p|^2]^{1/2}$, $A_2 = -\Omega_c^*\Omega_p A_1/D$, and $A_3 = d_2\Omega_p A_1/D$, with $D = |\Omega_c|^2 - d_2 d_3$ and $W = (|d_2|^2 + |\Omega_c|^2)/|D|^2$. Then Eqs. (3) and (5) are reduced to the following (2+1)-D NLS equation with saturation nonlinearity:

$$i\frac{\partial\Omega_p}{\partial z} + \frac{c}{2\omega_p}\left(\frac{\partial^2}{\partial x^2} + \frac{\partial^2}{\partial y^2}\right)\Omega_p + \kappa\frac{d_2\Omega_p}{D(1+W|\Omega_p|^2)} = 0. \tag{7}$$

In linear regime, the last term of Eq. (7) is reduced into $\kappa d_2 \Omega_p / D$ and hence one gets a linear (2+1)-D Schrödinger equation. For a Gaussian input of the probe field, this equation admits the solution

$$\Omega_p = \frac{\Omega_p(0)}{1 + 2iz/(k_p w_0^2)} \exp\left[-\left(\frac{x^2 + y^2}{w_0^2 + 2iz/k_p} \right) \right] \exp\left(i\kappa \frac{d_2}{D} z \right), \tag{8}$$

where $\Omega_p(0)$ (w_0) is the amplitude (minimum radius) of the probe beam at $z=0$. It is obvious that, with increasing z, the amplitude (radius) of the beam decreases (increases) due to the diffraction effect, represented by $(\partial^2/\partial x^2 + \partial^2/\partial y^2)$ in Eq. (8). In order to get a stable (i.e., diffraction-free) (2+1)-D probe beam one should find an effective remedy to cancel this detrimental diffraction effect. This is the main objective of the next section.

III. HIGH-DIMENSIONAL SPATIAL OPTICAL SOLITONS AND THEIR STABILITY AND CONTROLLABILITY

In the last section, we have shown that a linear (2+1)-D probe optical beam is unstable during propagation. We now demonstrate that the effects of saturation nonlinearity and the EIT of the system can be used to obtain a stable (2+1)-D spatial optical soliton.

A. (2+1)-D spatial soliton solutions and their stability

For a weak probe field, one can expand the last term on the left-hand side of Eq. (7) with respect to Ω_p to the second order and hence obtain a NLS equation with cubic nonlinearity,

$$i\frac{\partial \Omega_p}{\partial z} + \frac{c}{2\omega_p}\left(\frac{\partial^2}{\partial x^2} + \frac{\partial^2}{\partial y^2} \right)\Omega_p + \frac{\kappa d_2}{D}(1 - W|\Omega_p|^2)\Omega_p = 0. \tag{9}$$

It is well known that the plane soliton solution of this equation is unstable [2]. Thus in order to get a shape-preserving probe beam we must include the saturation nonlinearity of the system. In this case the nonlinear refractive index, defined by $\chi = (2c\kappa d_2/\omega_p D)(1 + W|\Omega_p|^2)^{-1}$, contains infinite many terms with both self-focusing and self-defocusing nonlinearities. This point can easily be seen by making a Taylor expansion for χ with respect to probe-light intensity. As will be shown later, it is just this property that can be used to avoid the collapse of the probe beam and hence a stable (2+1)-D spatial optical soliton is possible in the system.

We now study the soliton solution of Eq. (7). For a clear demonstration, we introduce dimensionless variables $s = L_{\text{diff}}^{-1} z$, $(\zeta, \eta) = R_\perp^{-1}(x, y)$, and $u = U_0^{-1}\Omega_p$, where $L_{\text{diff}} = \omega_p R_\perp^2 / c$, $R_\perp$, and $U_0 = 1/\sqrt{W}$ are the characteristic diffraction length, beam radius, and Rabi frequency of the probe field, respectively. With these variables, Eq. (7) can be written as the dimensionless form,

$$i\frac{\partial u}{\partial s} + \frac{1}{2}\left(\frac{\partial^2}{\partial \zeta^2} + \frac{\partial^2}{\partial \eta^2} \right)u + \frac{au}{1 + |u|^2} = 0, \tag{10}$$

where $a = \kappa d_2 L_{\text{diff}}/D \equiv a_R + ia_I$, with $a_R = \kappa L_{\text{diff}} \Delta_2 (|\Omega_c|^2 - \Delta_2\Delta_3)/[(|\Omega_c|^2 - \Delta_2\Delta_3)^2 + \Delta_2^2(\gamma_3^{\text{AV}})^2]$ and $a_I = \kappa L_{\text{diff}} \Delta_2^2 \gamma_3^{\text{AV}} / [(|\Omega_c|^2 - \Delta_2\Delta_3)^2 + \Delta_2^2(\gamma_3^{\text{AV}})^2]$ [20]. One recognizes that $a_I \propto \Delta_2^2$ when $|\Omega_c|^2 - \Delta_2\Delta_3 \neq 0$, and thus a_I can be greatly suppressed if Δ_2 is sufficiently small.

As a first step, we assume $a_I \ll a_R$ and only reserve the real part of a. This means the absorption of the medium plays no significant role and the system can be approximately taken as conservative. Actually, such a case is possible with the coupling field being strong enough (i.e., under the EIT configuration) and a realistic parameter set is suitably chosen (see the example given below). We introduce the transformation $u = v \exp(ia_R s)$ and assume that the solution is cylindrically symmetric with the form $v(s, r = \sqrt{\zeta^2 + \eta^2}) = \exp(i\beta s)\psi(r)$, where β is a real wave number and $\psi(r)$ is a real function describing the radial behavior. Then Eq. (10) is reduced into

$$\frac{\partial^2 \psi}{\partial r^2} + \frac{1}{r}\frac{\partial \psi}{\partial r} - 2\psi\left(\frac{a_R \psi^2}{1 + \psi^2} + \beta \right) = 0. \tag{11}$$

We determine the magnitude of β by choosing the peak soliton amplitude $\psi(s=0) = \psi_0$. The boundary conditions are $\partial\psi/\partial r = 0$ at $r=0$ and $\partial\psi/\partial r = \psi = 0$ at $r \to \infty$. We change the values of β and numerically integrate Eq. (11) until the computed spatial profile $\psi(r)$ satisfies the given boundary conditions. The calculating result on several soliton profiles corresponding to different peak values has been shown in Fig. 2(a). We see that the soliton's beam size varies inversely with its field amplitude. Both the value of β and the total power increase as the peak soliton intensity increases.

We now investigate the stability of the (2+1)-D spatial soliton against small perturbations by using well-known Vakhitov-Kolokolov (VK) criterion [15]. Shown in Fig. 2(b) is the numerical curve of the power $P = 2\pi \int_0^\infty \psi(r)^2 r dr$ contained in each soliton, versus the parameter β. We see that in each point of the curve we have $\partial P/\partial\beta > 0$. According to the VK criterion, this proves that the (2+1)-D spatial optical soliton obtained is stable.

The above calculating result is obtained by neglecting the absorption of the medium, i.e., a_I has been taken as zero. We now give a practical numerical example to show that such a situation can indeed be possible under the EIT condition. We consider a system working with ultracold ^{85}Rb alkali atomic gas (for canceling Doppler broadenings and shifts), in which $|5S_{1/2}, F=2\rangle$, $|5S_{1/2}, F=3\rangle$, and $|5P_{1/2}, F=2\rangle$ are selected as the states $|1\rangle$, $|2\rangle$, and $|3\rangle$, respectively. In this system one can have the decay rates $\gamma_2^{\text{AV}} \approx 1$ kHz and $\gamma_3^{\text{AV}} \approx 5.9$ MHz [21]. If taking $\kappa = 6.0 \times 10^9$ cm^{-1} s^{-1}, $\Omega_c = 1.0 \times 10^7$ s^{-1}, $\Delta_2 = 2.0 \times 10^5$ s^{-1}, $\Delta_3 = 1.0 \times 10^9$ s^{-1}, $\lambda_p = 800$ nm (the wavelength of the probe field), and $R_\perp = 40$ μm, we obtain the diffraction length $L_{\text{diff}} \simeq 1.25$ cm, $U_0 \simeq 1.0 \times 10^7$ s^{-1}, and $a \simeq -15.08 + 0.18i$. Thus the imaginary part of a is about 80 times smaller than the real part and hence can be neglected or taken as a small perturbation [22]. Although the Vakhitov-Kolokolov criterion holds only for a conservative limit, we

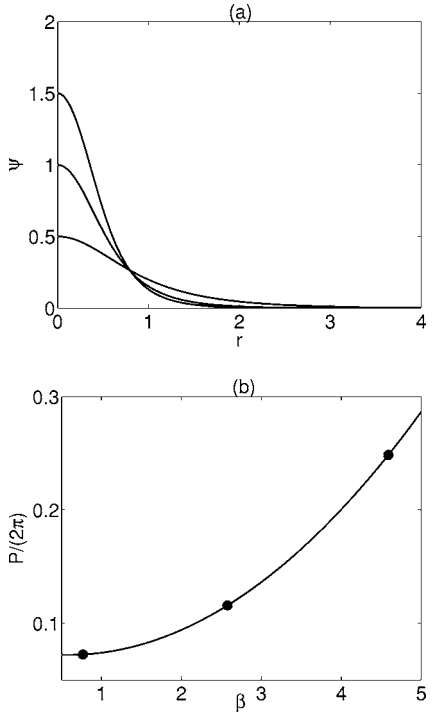

FIG. 2. (a) Soliton profiles with a cylindrical symmetry calculated by numerical integrations of Eq. (11) with $a_R=-15.1$. The profiles from top to bottom have peak values 1.5, 1.0, and 0.5, and corresponding values of β are 4.6, 2.6, and 0.8, respectively. (b) The power P contained in each soliton vs the parameter β.

expect that a very small dissipative perturbation will induce only a small deformation of the spatial soliton.

We now consider the evolution and stability of (2+1)-D spatial optical solitons during propagation by taking $s=z/L_{\text{diff}}$ as a "time" coordinate. We try to get a (2+1)-D spatial soliton solution by a direct numerical integration starting from Eq. (10). In our calculation, the split-step Fourier method is used to propagate an initial condition. The soliton stability and convergence are examined by propagating an initial Gaussian beam with a similar intensity and beam width as shown in Fig. 2, which has the form $u=0.7\exp[-(\zeta^2+\eta^2)]$. In Fig. 3, we plot the intensity of the probe field $|u|^2=|\Omega_p/U_0|^2$ versus s axis. The beam's center locates at the origin of the x-y plane. Panel (a) shows the initial Gaussian beam, which evolves into a spatial soliton when $s>1$ (i.e., $z>L_{\text{diff}}=1.25$ cm). Shown in panel (b) is the result of the spatial soliton at $s=2.5$ (i.e., $z=3.1$ cm) without considering absorption (i.e., by neglecting small a_I). The physical reason for the shape-preserving propagation with the form of the high-dimensional spatial soliton is due to the balance between the saturation nonlinearity and the diffraction of the system. The peak intensity $|u|^2$ versus s is given by the solid curve in panel (d). We see that there exists a breathing of the peak intensity before converging to a constant peak value (≈ 0.7). This breathing can be made smaller if the initial state is selected more closely to an exact soliton solution. With our parameters the peak power of the spatial soliton in panel (b) is 1.2×10^{-5} mW, which corresponds to the peak intensity $I_p=2.3\times10^{-4}$ W cm^{-2}. We see that in the

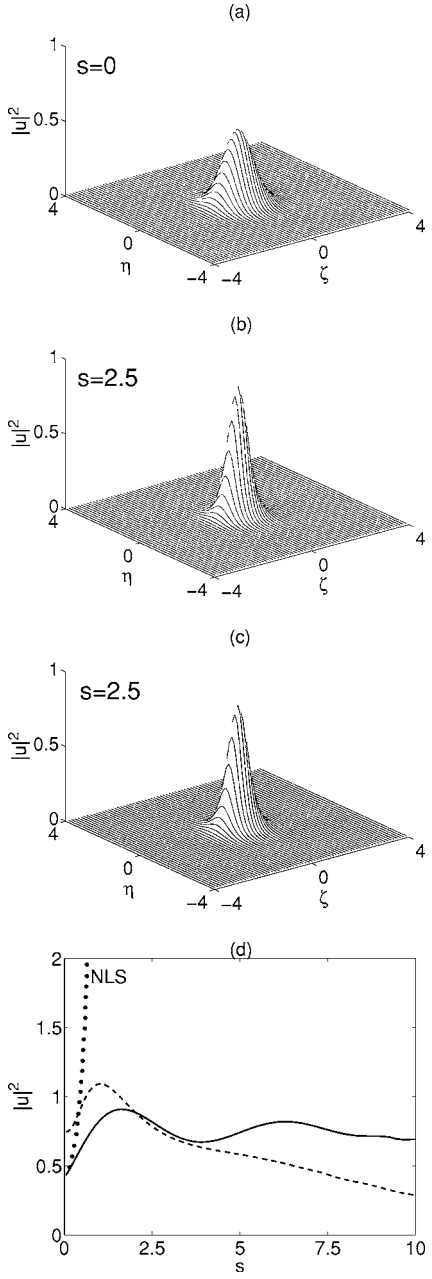

FIG. 3. Beam propagation through an atomic cell. (a) The initial (Gaussian) beam. (b) The beam at $s=2.5$ (i.e., $z=3.1$ cm) without considering absorption. (c) The beam at $s=2.5$ in the presence of absorption. (d) The curve of intensity vs s. The solid (dashed) line denotes the case without (with) the effect of absorption. The beam breathes as it converges to a soliton. In the region $0\leq s\leq 5$, the difference between two curves is very small. The curve (dotted line) with a system offering no saturation is also plotted.

EIT-based system *extremely* low input power is needed for generating (2+1)-D spatial optical solitons in such a highly resonant atomic medium, which is drastically different from the conventional technique of the spatial optical soliton generation in a waveguide where an input laser pulse with very high peak power ($\sim 10^2$ kW) is needed in order to bring out a sufficient nonlinear effect [24].

Though the absorption can be largely suppressed by the EIT effect, it displays an influence on the spatial soliton. In panel (c) of Fig. 3 we have shown the result of the spatial soliton at $s=2.5$ (i.e., $z=3.1$ cm) in the presence of absorption by including a small imaginary part of the parameter a in Eq. (10). We see that, comparing with the case without absorption [i.e., the result given by Fig. 3(b)], there is indeed a small damping on the spatial soliton, which induces a decrease of soliton amplitude and an increase of soliton width. To get a more clear picture for such a damping effect for different propagating distance s, we have plotted the peak intensity of the spatial soliton $|u|^2$ in the case of the absorption, given by the dashed line in Fig. 3(d). We see that for small s the difference between the soliton amplitudes with (the dashed curve) and without (the solid curve) the absorption is not significant; while for a longer propagating distance (i.e., $s>5$ or $z>6.25$ cm), the damping of the peak intensity becomes obvious. Thus in a distance shorter than $z=6.25$ cm, a spatial soliton with a small deformation during propagation could be observed experimentally in the system.

For comparison, we have also studied the propagation of a spatial soliton in the absence of the saturation nonlinearity. In this case the envelope of the probe field is governed by the cubic NLS equation (9). The result of the peak intensity of the soliton as a function of s has been plotted as the dotted line in Fig. 3(d). We see that for such a (2+1)-D spatial soliton an inevitable collapse occurs in a very short propagating distance. Consequently, in order to form a stable (2+1)-D spatial soliton in the system one needs not only the EIT-based quantum interference effect, which suppresses largely the absorption, but also the saturation nonlinearity, which arrests the collapse during the propagation of the optical beam.

At the end of this subsection we turn to consider the quantity P_{loss} defined by Eq. (6). After taking $\Omega_p=0.8\Omega_c$ and the length of the atomic cell $s=2.5$ (i.e., $z=3.1$ cm), we get $P_{\text{loss}}\approx 0.16$, which shows that the incoherent processes in our system are indeed less important.

B. Interactions between spatial optical solitons

Now we proceed with an investigation on the interaction between two spatial optical solitons in our system. For the particular case of only one transverse dimension and with only cubic nonlinearity, Eq. (10) is reduced to a (1+1)-D NLS equation, which admits analytical soliton solutions. The interaction between two solitons in such a simple system has been widely studied in literature both analytically and numerically. It has been found that the interaction property depends on the relative amplitudes and relative phases of the solitons [1,2].

For the case of high dimensions and with saturation nonlinearity, the study of the interaction among solitons is difficult because an analytical high-dimensional soliton solution is not available up to now. Thus one must resort to numerical simulation to get useful information on soliton interactions. Of course the knowledge of the (1+1)-D soliton interaction obtained before [1,2] can be taken as a guide for the high-dimensional case.

We have made a numerical study on the collision between two (2+1)-D spatial optical solitons. We found that the collision property of solitons in saturable nonlinear optical media are more rich and interesting than those found in cubic nonlinear media. The reason is that our system is a saturable nonlinear medium, which supports (2+1)-D solitons and allows soliton collisions in full three dimensions. New phenomena such as soliton fusion, fission, and annihilation can occur, such as that found in a previous study with a different physical stem [23]. The initial condition in our simulation consists of two Gaussian beams, which reads

$$u(0,\zeta,\eta)=A_{m1}\exp\{-[\zeta^2+(\eta-s_0/2)^2]\}\exp(-i\eta+i\phi_1)+A_{m2}\exp\{-[\zeta^2+(\eta+s_0/2)^2]\}\exp(i\eta+i\phi_2). \tag{12}$$

The property of the interaction between two (2+1)-D spatial optical solitons is determined by the initial relative amplitudes ($\Delta A=A_{m1}-A_{m2}$) and relative phases ($\delta\phi=\phi_1-\phi_2=\pi$). Here we only present the results on the collision between two solitons with equal amplitudes (i.e., $A_{m1}=A_{m2}=0.7$). Shown in Fig. 4(a) is the result of an elastic collision between two solitons with an initial relative phase $\Delta\phi=\pi$. The initial separation is taken as $s_0=0.16$ and the convergent input angle is $\theta\simeq 4.3\times 10^{-3}$ rad. The three-dimensional plot shown in the figure is generated by taking $\zeta=0$ ($\eta=r$) for each value of s and two input beams propagate to each other along the η axis. From the figure we see that in this case the interaction between two spatial solitons is repulsive. The physical reason is that the refractive index in the central region of the interaction is lowered due to the overlap of the two solitons. The emerging waveform breathes after the interaction and then converges to respective solitons. We see that a small phase (position) shift occurs for each soliton after the collision.

Figure 4(b) reports the result of an inelastic collision between two spatial optical solitons, which occurs for the relative phase $\Delta\phi=0$. The separation and colliding angle of the two solitons are chosen the same as in Fig. 4(a). In this situation the intensity in the central region of the collision is increased by the overlap of the solitons due to attractive interaction, which leads to an increase of the refractive index and hence attracts more light to the central region. As a result, two solitons attract each other and undergo a fusion. The emerging wave form breathes just after the collision and then converges to a single soliton with an internal oscillation in its amplitude.

A variation of the colliding angle θ of two solitons can also result in a change of interaction property. In Fig. 4(c) we have shown the numerical result by keeping $\Delta\phi=0$ but increasing the colliding angle to $\theta\simeq 6.4\times 10^{-3}$ rad. We see that two solitons nearly disappear after their collision. This is due to the reason that in this case the diffraction effect is dominant over the self-focusing of the system. Figure 4(d) shows the result of a collision by a further increase of the colliding angle. In this situation two solitons pass through each other with decreased (increased) amplitudes (widths).

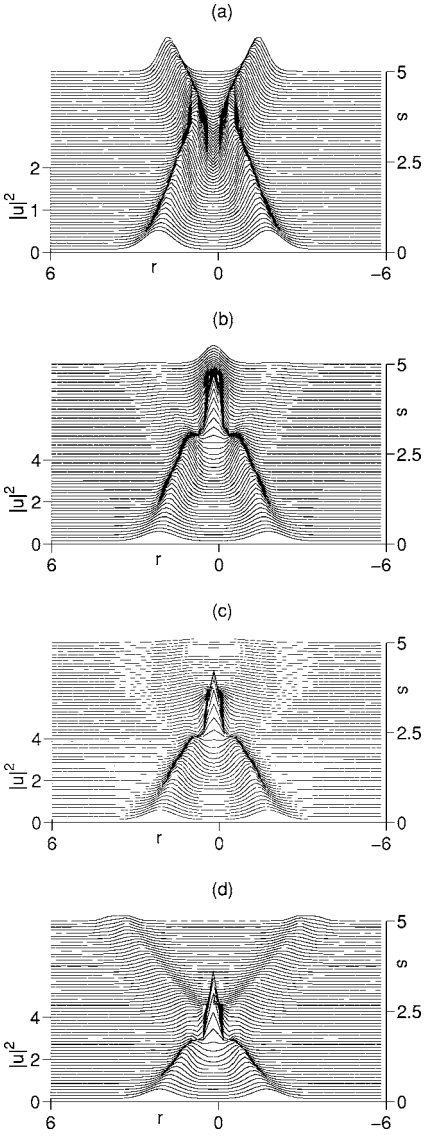

FIG. 4. The interactions between two spatial solitons with identical intensity. (a) The elastic collision of two solitons. The initial relative phase $\Delta\phi=\pi$, separation is $s_0=0.16$, and the angle of the collision is $\theta\simeq 4.3\times 10^{-3}$ rad. (b) The inelastic collision with $\Delta\phi=0$. The solitons collide and fuse into one. (c) The case when increasing θ to about 6.4×10^{-3} rad. Two solitons nearly disappear after a collision. (d) The case when θ increases further. The two solitons pass through each other.

C. Controllability of spatial optical solitons

As shown above, stable (2+1)-D spatial optical solitons can occur in the three-state Λ system under the EIT condition. The formation of these nonlinear localized structures is due to the atomic coherence via the EIT that suppresses absorption and the balance between beam diffraction and saturation nonlinearity that create a nonlinear waveguide. In this subsection we show that such spatial optical solitons can be controlled by manipulating the parameters of the system. One of the important parameters is the intensity of coupling laser, which can be used to adjust the physical property of the nonlinear waveguide formed. For our three-level system

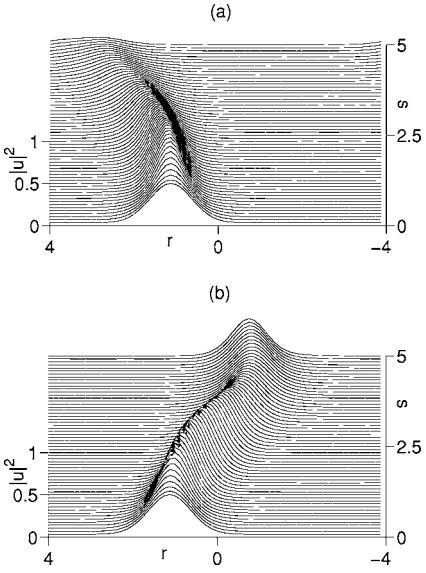

FIG. 5. (a) The trajectory of the soliton for $\Omega_c=1.0\times 10^7\times\exp[-(x^2+y^2)/36]$ s^{-1}. The soliton propagates into the lower coupling intensity regime and will be absorbed soon. (b) The trajectory of soliton for $\Omega_c=5.0\times 10^7(\mathcal{L}_{00}+\mathcal{L}_{20}+0.1)$ s^{-1} ($\mathcal{L}_{pm}$ is the normalized LG modes). The soliton is restricted in the center of the coupling beam.

the refractive index induced by the coupling beam is given by

$$n_p = 1 + c\,\mathrm{Re}[K(\omega)]/\omega_p = 1 + c\kappa\Delta_2/\omega_p(|\Omega_c|^2 - \Delta_2\Delta_3) \tag{13}$$

for $\Delta_2 \gg \gamma_2^{\mathrm{AV}}$ and $\Delta_3 \gg \gamma_3^{\mathrm{AV}}$. Here $K=K(\omega)$ is the linear dispersion relation of the system, whose expression can be obtained by setting $A_1=1$, $A_j=\tilde{A}_j\exp\{i[K(\omega)z-\omega t]\}$ $(j=2,3)$ and $\Omega_p=\tilde{\Omega}_p\exp\{i[K(\omega)z-\omega t]\}$, with $\tilde{A}_j$, $\tilde{\Omega}_p$, and Ω_c being slowly varying functions of z and t. Substituting them into Eqs. (3), we readily obtain $K(\omega)=\omega/c+\kappa(\omega+d_2)/(|\Omega_c|^2-d_2d_3)$. It is obvious that one can easily control the refractive index n_p and realize the controllability of the soliton trajectory by manipulating Ω_c.

Specifically, we assume that the envelope of the coupling light beam is not a constant but a Gaussian profile with the form $\Omega_c=1.0\times 10^7\exp[-(\zeta^2+\eta^2)/36]$ s^{-1} [25]. Shown in Fig. 5(a) is our numerical result of a spatial optical soliton with such a coupling beam. In the simulation, a small initial displacement of the soliton's center from the position of the maximum of the coupling beam has been introduced. Note that the maximum of the coupling beam is at $r=0$. From the figure we see that the soliton propagates into the region where the intensity of the coupling field is smaller (i.e., the region with a larger refractive index). However, at the boundary of the coupling beam, the effect of absorption increases fast. As a result, the soliton is absorbed soon toward the boundary of the coupling beam.

We can alter the transversal profile of the coupling beam to exert different effects on the spatial soliton. As another example, we consider a beam profile that takes the form of

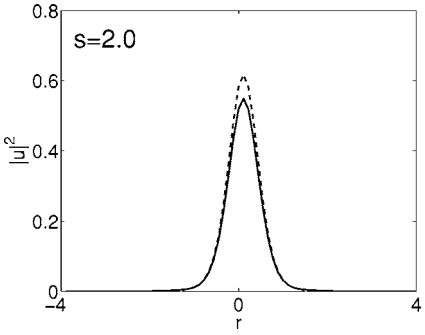

FIG. 6. Spatial optical solitons at $s=1.0$ ($z=2.5$ cm) calculated from Eq. (10) (the solid line) and from Eqs. (3) and (5) (the dashed line).

an optical bottle, which is considered to be a superposition of two coaxial Laguerre-Gaussian (LG) beams. Specifically, we take $\Omega_c=5.0\times10^7(\mathcal{L}_{00}+\mathcal{L}_{20}+0.1)$ s^{-1}. In cylindrical coordinates the normalized LG mode at the beam waist is given by [26]

$$\mathcal{L}_{pm}(r,\phi)=\sqrt{\frac{4p!}{(1+\delta_{0m})\pi(p+|m|)!}}L_p^{|m|}\left(\frac{2r^2}{w_0^2}\right)\left(\frac{\sqrt{2}r}{w_0}\right)^{|m|}\times\frac{1}{w_0}\exp(-r^2/w_0^2)\exp(im\phi), \tag{14}$$

where $L_p^{|m|}(r)$ are the associated Laguerre polynomials. The index p is the number of nonaxial radial nodes of the mode and m is referred to as the winding number. For simplicity, in our simulation $m=0$ is chosen. The propagation of the spatial soliton under such a LG coupling beam is shown in Fig. 5(b). We see that in this case the during propagation soliton is restricted in the central region of the coupling beam and undertakes only a small absorption within the propagation distance $z=6.25$ cm.

IV. DISCUSSION AND SUMMARY

The results for the stable (2+1)-D spatial optical solitons presented above are based on nonlinear envelope Eq. (10). For a better confirmation of our theoretical approach, it is necessary to check the stability of the spatial optical solitons starting directly from the Maxwell-Schrödinger Eqs. (3) and (5). We have performed an additional numerical simulation and the result for a single spatial optical-soliton solution has been provided in Fig. 6. In the figure, the solid line is the soliton profile by using Eq. (10) and the dashed line is the profile by using Eqs. (3) and (5). We see that up to $s=2.0$ (i.e., $z=2.5$ cm) both soliton shapes remain coincident except for a small decrease of soliton amplitude due to a small absorption of the medium.

In conclusion, we have studied the formation and propagation of stable (2+1)-D spatial optical solitons in a resonant three-level atomic system. From the equations of motion describing the evolution of atomic amplitudes and the probe field, we have obtained a NLS equation with a saturation nonlinearity, which governs the dynamics of the envelope of the probe field. We have shown that, due to the quantum interference effect induced by the coupling laser field, the absorption of the probe field is largely suppressed and the saturation nonlinearity can arrest the collapse of the probe beam. As a result, the system can support (2+1)-D spatial optical solitons under the EIT condition. We have demonstrated that the spatial optical soliton in such a system can be generated by using an extremely weak probe-light intensity. The stability of the spatial optical soliton has been confirmed by using the Vakhitov-Kolokolov criterion and a cross-checked numerical calculation with examples of realistic physical parameters. We have also made a detailed study on the interaction between two (2+1)-D spatial optical solitons. We have found that the property of the soliton interaction depends on the initial relative amplitudes and relative phases, as well as the colliding angle. The controllability of the spatial optical soliton has been studied by manipulating the coupling laser field. In addition, for testing our theory we have also presented a numerical simulation for the (2+1)-D spatial soliton starting directly from the Maxwell-Schrödinger equations. The results presented in this work may be useful for guiding an experimental finding of stable (2+1)-D spatial weak-light solitons in resonant atomic systems and have potential applications in modern optical information processing and engineering.

ACKNOWLEDGMENTS

This work was supported by the Key Development Program for Basic Research of China under Grant No. 2005CB724508, NSF-China under Grant Nos. 10434060, 90403008, and 10674060, and the Ph.D. Program Scholarship Fund of ECNU 2006.

APPENDIX: EQUATIONS OF MOTION FOR DENSITY MATRIX

The interaction between atoms and optical fields for our three-level system can be described by density-matrix equations

$$\dot{\rho}_{11}=\Gamma_{31}\rho_{33}+i(\Omega_p^*\rho_{31}-\text{c.c.})-\gamma_1\rho_{11}, \tag{A1a}$$

$$\dot{\rho}_{22}=\Gamma_{32}\rho_{33}+i(\Omega_c^*\rho_{32}-\text{c.c.})-\gamma_2\rho_{22}, \tag{A1b}$$

$$\dot{\rho}_{33}=-(\Gamma_{31}+\Gamma_{32}+\gamma_3)\rho_{33}-i(\Omega_p^*\rho_{31}-\text{c.c.})-i(\Omega_c^*\rho_{32}-\text{c.c.}), \tag{A1c}$$

$$\dot{\rho}_{12}=-(\gamma_{12}/2+\gamma_{12}^{\text{col}}+i\Delta_2)\rho_{12}+i\Omega_p^*\rho_{32}-i\Omega_c\rho_{13}, \tag{A1d}$$

$$\dot{\rho}_{13}=-[(\gamma_{13}+\Gamma_{31}+\Gamma_{32})/2+\gamma_{13}^{\text{col}}+i\Delta_3]\rho_{13}+i\Omega_p^*(\rho_{33}-\rho_{11})-i\Omega_c^*\rho_{12}, \tag{A1e}$$

$$\dot{\rho}_{23}=-[(\gamma_{23}+\Gamma_{31}+\Gamma_{32})/2+\gamma_{23}^{\text{col}}+i\Delta_{32}]\rho_{23}-i\Omega_p^*\rho_{21}+i\Omega_c^*(\rho_{33}-\rho_{22}), \tag{A1f}$$

with $\Delta_{32}=\Delta_3-\Delta_2$, $\gamma_{jl}=\gamma_j+\gamma_l$. Here Γ_{ij} denotes the spontane-

ous emission decay rate from state $|i\rangle$ to state $|j\rangle$ and γ_j is the ionization rate of the state $|j\rangle$. γ_{jl}^{col} represents the dipole dephasing rate reflecting the loss of phase coherence without a change of population, as might occur with elastic collisions [27]. From Eqs. (A1a)–(A1c), one has $\Sigma_{j=1}^{3}\dot{\rho}_{jj}=-\Sigma_{j=1}^{3}\gamma_j\rho_{jj}$ and hence the system is open.

Since in our system the states $|1\rangle$ and $|2\rangle$ are two hyperfine ground states, one has a vanishing γ_1 and a small γ_2. On the other hand, due to the quantum interference (i.e., EIT) effect induced by the coupling laser field Ω_c, the absorption of the probe field is largely canceled and hence the system keeps almost in the dark state $|1\rangle$ if its initial state is prepared in this dark state. Therefore, during the evolution of the system one has $\Sigma_{j=1}^{3}|A_j|^2\approx 1$ with $A_1\approx 1$ and $|A_2|,|A_3|\ll|A_1|$ for any time t.

It can be shown that, for an EIT-based partially open system, the AV approach and the density-matrix equation approach are roughly equivalent [16,17]. For providing a relation between two descriptions given by Eqs. (3) and (A1), we have compared the linear susceptibilities obtained by using two different approaches as done in Ref. [17]. The results show that the phenomenological decay rates γ_j^{AV} in state $|j\rangle$ introduced in the amplitude equations (3) can be appropriately interpreted as

$$\gamma_2^{\text{AV}} \leftrightarrow \frac{1}{2}\gamma_{12}+\gamma_{12}^{\text{col}}, \quad \gamma_3^{\text{AV}} \leftrightarrow \frac{1}{2}(\Gamma_{31}+\Gamma_{32}+\gamma_{13})+\gamma_{13}^{\text{col}}. \tag{A2}$$

[1] G. P. Agrawal, *Nonlinear Fiber Optics* (Elsevier (Singapore) Pte Ltd., Singapore, 2004).

[2] A. Hasegawa and Y. Kodama, *Solitons in Optical Communications* (Clarendon, Oxford, 1995), and references therein.

[3] Y. S. Kivshar and B. Luther-Davies, Phys. Rep. **298**, 81 (1998), and references therein.

[4] G. I. Stegeman and M. Segev, Phys. Today **51**, 8, 42 (1998); G. I. Stegeman and M. Segev, Science **286**, 1518 (1999).

[5] S. E. Harris, Phys. Today **50**, 7, 36 (1997).

[6] M. D. Lukin, Rev. Mod. Phys. **75**, 457 (2003), and references therein.

[7] M. Fleischhauer, A. Imamoglu, and J. P. Marangos, Rev. Mod. Phys. **77**, 633 (2005), and references therein.

[8] L. Deng *et al.*,Phys. Rev. Lett. **88**, 143902 (2002).

[9] M. Xiao *et al.*, Phys. Rev. Lett. **74**, 666 (1995); H. Kang and Y. Zhu, Phys. Rev. Lett. **91**, 093601 (2003).

[10] T. Hong, Phys. Rev. Lett. **90**, 183901 (2003).

[11] H. Michinel, M. J. Paz-Alonso, and V. M. Pérez-García, Phys. Rev. Lett. **96**, 023903 (2006).

[12] Y. Wu and L. Deng, Phys. Rev. Lett. **93**, 143904 (2004); Y. Wu and L. Deng, Opt. Lett. **29**, 2064 (2004).

[13] G. Huang, L. Deng, and M. G. Payne, Phys. Rev. E **72**, 016617 (2005); L. Deng, M. G. Payne, G. Huang, and E. W. Hagley, *ibid.* **72**, 055601 (R) (2005).

[14] C. Hang, G. Huang, and L. Deng, Phys. Rev. E **73**, 036607 (2006); G. Huang, K. Jiang, M. G. Payne, and L. Deng, *ibid.* **73**, 056606 (2006).

[15] M. G. Vakhitov and A. A. Kolokolov, Izv. Vyssh. Uchebn. Zaved., Radiofiz. **16**, 1020 (1973) [Sov. J. Radiophys. Quantum Electron. **16**, 783 (1973)].

[16] Z. Dutton, Ph.D. thesis, Harvard University, 2002 (unpublished).

[17] C. Ottaviani *et al.*, e-print physics/0510200.

[18] S. E. Harris *et al.*, Phys. Rev. Lett. **64**, 1107 (1990); S. E. Harris, *ibid.* **72**, 52 (1994); J. H. Eberly, Quantum Semiclassic. Opt. **7**, 373 (1995); S. E. Harris and Z.-H. Luo, Phys. Rev. A **52**, R928 (1995); H. Schmidt and A. Imamoglu, Opt. Lett. **21**, 1936 (1996); S. E. Harris and Y. Yamamoto, Phys. Rev. Lett. **81**, 3611 (1998); D. Petrosyan and G. Kurizki, Phys. Rev. A **65**, 033833 (2002).

[19] By taking $t=t'\tau_0$, where t' is dimensionless time and τ_0 is the characteristic temporal width of the envelope of the probe field, the first term of Eqs. (3a) and (3b) is transferred into the dimensionless form $i(\partial/\partial t'+d_j\tau_0)A_j$ $(j=2,3)$. Consider, for example, a cold atom system having a decay rate γ_3^{AV} around 10 MHz (γ_2^{AV} can be much less this value). If Δ_j is chosen to be larger than 1.0×10^6 s^{-1} and τ_0 is around 10^{-5} s, one has $|d_j|\tau_0>10$ and hence the time-derivative terms in Eqs. (3a) and (3b) play no significant role.

[20] Since γ_2^{AV} is small (e.g., for cold atoms it can be less than 10^3 Hz) we shall neglect it for simplicity in the following paper.

[21] Y. Wu, J. Saldana, and Y. Zhu, Phys. Rev. A **67**, 013811 (2003).

[22] We should mention that $a_R<0$ is a necessary condition for Eq. (10) to provide a self-focusing effect for low probe amplitude and a self-defocusing effect for higher probe amplitude. Thus $|\Omega_c|^2-\Delta_2\Delta_3<0$ should be selected.

[23] S. Gatz and J. Herrmann, IEEE J. Quantum Electron. **28**, 1732 (1992).

[24] J. S. Aitchison *et al.*, Opt. Lett. **15**, 471 (1990).

[25] The radius of the control light should be large in order to make the derivation of Eqs. (3) and (5) valid. In the simulation such a radius is six times the width of the probe beam.

[26] T. Freegarde and K. Dholakia, Phys. Rev. A **66**, 013413 (2002).

[27] B. W. Shore, *The Theory of Coherent Atomic Excitations* (John Wiley & Sons, New York, 1992), Chap. 22.